Transition to Higher Chaos in Diffusively Coupled Chemical Oscillators *

Gerold Baier, Sven Sahle, Ursula Kummer, and Roland Brock
Institute for Chemical Plant Physiology, University of Tübingen, D-72076 Tübingen, FRG

Z. Naturforsch. **49a**, 835–837 (1994); received May 30, 1994

A one-dimensional array of diffusively coupled identical oscillators is considered. It is demonstrated that coupling of two, three, four, and six oscillators can create chaos with one, two, three, and four positive Lyapunov characteristic exponents, respectively. We suggest that the turbulent behavior found with many coupled cells can be explained in terms of a high-order chaotic attractor.

1. Introduction

Highly irregular spatio-temporal behavior in reaction-diffusion systems is often referred to as chemical turbulence [1]. Rössler proposed that one possible road to turbulence is via the chaotic hierarchy, i.e., with stepwise increasing number of positive Lyapunov characteristic exponents (LCEs) in finite-dimensional systems [2]. He showed that two diffusively coupled nonlinear oscillators were not only able to break symmetry as proposed by Turing but also were able to oscillate chaotically [1]. Obviously one way to study the transition from homogeneous oscillations to spacetime turbulent behavior is to search for chaotic hierarchies in chemical reactions with increasing number of degrees of freedom.

A simple way to model a spatial degree of freedom in unstirred chemical reactions is diffusive coupling of a one-dimensional array of cells with homogeneous kinetics. Usually many such cells are simulated numerically to approach the limit of the infinite-dimensional partial differential equations governing the dynamics in space and time. However, small volumes of diffusively stirred systems, or few diffusively coupled stirred flow reactors can be described by a finite number of cells. Here, we restrict ourselves to these finite-dimensional problems and study arrays of cells with up to 50 members and focus on the temporal and (discrete) spatial instabilities with periodic boundary conditions.

* Paper presented at the 4th Annual Meeting of ENGADYN, Grenoble, October 11–14, 1993.

Reprint requests to Dr. G. Baier, Institut für Chemische Pflanzenphysiologie, Universität Tübingen, Corrensstraße 41, D-72076 Tübingen.

2. The Model

A single model compartment is assumed to obey homogeneous reaction kinetics. For the present study we use a simple two-variable scheme which allows oscillatory solutions:

$$\dot{X} = a + X\,Y - c_1\,X/(c_2 + X) = f_x, \qquad (1)$$
$$\dot{Y} = b - X\,Y = f_y,$$

whereby (X, Y, a, b, c_1, $c_2 \in \mathbf{R}$). There is a constant input to variable Y at rate b, and Y is turned to X with the aid of X (autocatalysis). This oscillator possesses a first-order autocatalytic term. Variable X is consumed in a reaction with Michaelis-Menten kinetics. At $a = 0.07$ there is a stable fixed point solution. Decreasing parameter a the fixed point loses stability at $a \approx 0.0655$, and a stable limit cycle is generated. The limit cycle increases in amplitude and stays stable as a is decreased down to zero.

The autocatalytic nonlinearity can easily be implemented in real systems using the reaction sequence $X + Y \rightarrow 2Z$, $Z \rightarrow X$, where the second step proceeds fast compared to the first. The Michaelis-Menten nonlinearity is the most common rate law to describe enzyme-controlled decay of substrate X. We therefore assume that this oscillator can be realized biochemically.

A closed one-dimensional array of oscillatory cells coupled by diffusion is written in the following way:

$$\begin{aligned}
\dot{X}_1 &= f_x + D_x(X_N + X_2 - 2X_1),\\
\dot{Y}_1 &= f_y + D_y(Y_N + Y_2 - 2Y_1),\\
\dot{X}_i &= f_x + D_x(X_{i-1} + X_{i+1} - 2X_i),\\
\dot{Y}_i &= f_y + D_y(Y_{i-1} + Y_{i+1} - 2Y_i),\\
\dot{X}_N &= f_x + D_x(X_1 + X_{N-1} - 2X_N),\\
\dot{Y}_N &= f_y + D_y(Y_1 + Y_{N-1} - 2Y_N),
\end{aligned} \qquad (2)$$

0932-0784 / 94 / 0900-0835 $ 06.00 © – Verlag der Zeitschrift für Naturforschung, D-72027 Tübingen

whereby ($X, Y, D_x, D_y \in \mathbf{R}$) and ($i \in \mathbf{N}, i = 2, \ldots (N-1)$; $N \geqq 3$ is the number of coupled cells. D_x and D_y are the diffusion coefficients of variables X and Y, respectively.

3. Results and Discussion

First, we consider two diffusively coupled oscillators (1):

$$\begin{aligned} \dot{X}_1 &= a + X_1 Y_1 - c_1 X_1/(c_2 + X_1) + D_x(X_2 - X_1), \\ \dot{Y}_1 &= b - X_1 Y_1 + D_y(Y_2 - Y_1), \\ \dot{X}_2 &= a + X_2 Y_2 - c_1 X_2/(c_2 + X_2) + D_x(X_1 - X_2), \\ \dot{Y}_2 &= b - X_2 Y_2 + D_y(Y_1 - Y_2). \end{aligned} \tag{3}$$

For constant parameter values $b = 0.12$, $c_1 = 0.5$, $c_2 = 0.1$, $D_x = 0.01$, $D_y = 0.001$ we vary parameter a and study the dynamics. As a is increased from zero there are large-amplitude oscillations and the two compartments are phase-locked ($0 < a < 0.051$).

For $0.055 < a < 0.066$ the stable attractor of (3) is a limit cycle with small-amplitude oscillations. In the intermediate region between the two limit cycles we find complex oscillations and chaos. As an example, at $a = 0.053$ we calculated the LCE spectrum of the four-variable system and found (0.008, 0, −0.375, −1.172) indicating a chaotic attractor with Lyapunov dimension $2 < D_L < 3$. In the case of chaotic oscillations the two compartments are out of phase, i.e. there is a loss of spatial symmetry compared to the case of the limit cycles.

Second, we take (2) and put $N = 3$. Thus we have a ring of three identical oscillators. Recording the dynamics as a function of increasing parameter a there is a transition from phase-locked large-amplitude oscillations to small-amplitude oscillations as in the case of two coupled cells. Again, under inspection of the transition region there is a finite range of parameter a in which the oscillations are either complex-periodic or aperiodic. From the bifurcation diagram we find that the transition from small-amplitude limit cycle to chaos for decreasing parameter a occurs via quasiperiodic motion on a two-torus. In the chaotic window we characterized attractors according to their LCE spectrum. There are either one or two positive LCEs, e.g. calculating the LCEs at $a = 0.053$ we find (0.023, 0.006, 0, −0.319) and thus hyperchaos with two positive exponents for the system with three coupled cells. The three cells show strong temporal and spatial irregularity.

For $N = 4$ in (2), the general picture of the dynamics is as for $N = 3$, i.e. a chaotic window is bracketed by large-amplitude and small-amplitude phase-locked oscillations. Looking now for the most complex case, the five largest LCEs in the chaotic window at $a = 0.052$ are calculated to be (0.035, 0.020, 0.005, 0, −0.264), and thus there is hyperchaos with three positive LCEs. For $N = 6$ the six largest LCEs in the chaotic window at $a = 0.052$ are (0.042, 0.029, 0.018, 0.009, 0, −0.011), and thus hyperchaos with four positive LCEs. These first results seem to indicate that a generation mechanism has been found which creates an increasing number of positive LCEs as the number of linearly coupled nonlinear oscillators is increased. We are therefore interested in the spatio-temporal behavior of systems with a larger number of cells in the transition region between the two spatially homogeneous (phase-locked) modes of oscillations.

For $N = 50$ in (2), as parameter a is decreased (e.g. starting from $a = 0.06$), we again observe a transition sequence from large-amplitude oscillations to complex behavior to small-amplitude oscillations. Incidentally, the window of complex behavior is approximately located at parameter values similar to the case of smaller N. As described above, there are quasiperiodic, complex-periodic and chaotic types of behavior in the complex window of parameter a. Particularly, the small-amplitude limit cycle loses stability via torus bifurcation to quasiperiodic motion. At the same time spatial coherence is lost. An example of the resulting quasiperiodic evolution in space and time is shown in Figure 1. At a lower value of parameter a the system settles to a higher chaotic state. Figure 2 presents an example of the highly irregular spatio-temporal evolution. A profile along the spatial coordinate is provided in Figure 3. We assume that the observed irregularity in this region of parameter space originates in the divergence due to positive Lyapunov exponents. These positive LCEs can result from diffusive coupling of oscillatory cells as demonstrated for few coupled cells above.

Diffusive coupling of chemical oscillators led to the numerical observation of a few steps of the chaotic hierarchy in our preliminary study. For the instances described the number of positive LCEs increased as the number of coupled cells was increased. We expect this tendency to continue. The most complex spatio-temporal behavior in the system of (2) with $N = 50$ would then be a highly chaotic attractor. However, at present the number of positive LCEs cannot be predicted merely from the dimension of the system. The

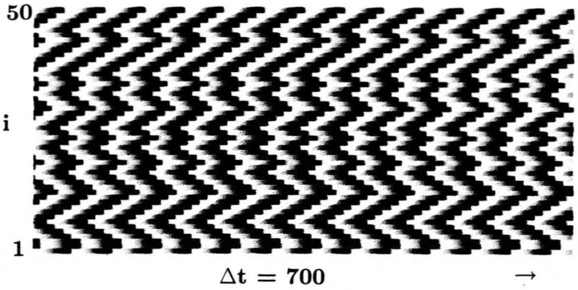

Fig. 1. Quasiperiodic time evolution of the system (2) with $N = 50$ and $a = 0.0541$. Grey coding of variables X_i from white (low values) to black (high values).

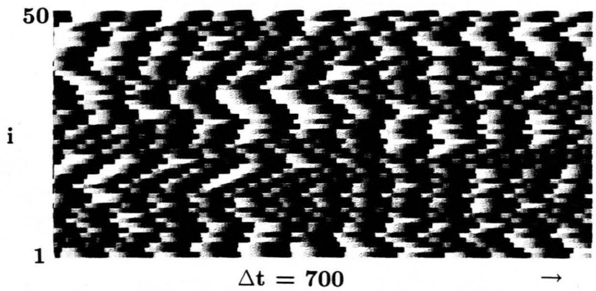

Fig. 2. Higher chaotic time evolution of the system (2) with $N = 50$ and $a = 0.053$. Grey coding of variables X_i as in Figure 1.

connection between new locally unstable directions in phase space and new directions of mean divergence on the attractor is unknown.

Another explicit model where an increase in dynamic complexity goes along with an increase in the available degrees of freedom was studied by Baier et al. [3]. In that case oscillating subsystems in a spatially homogeneous continuous flow reactor were coupled to a common feeding source. An increasing number of positive Lyapunov exponents was observed as the number of oscillators coupled to the source was increased. However, the present formulation using diffusive coupling of units enables one to apply the results from a system like (2) to spatially coupled cellular systems, e.g. in biology.

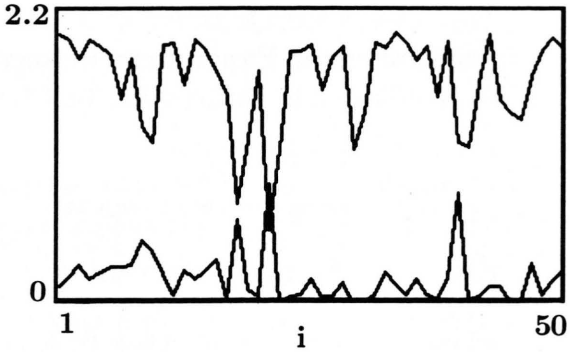

Fig. 3. Spatial distribution of concentrations of variables X_i (lower curve) and Y_i (upper curve) in (2) with parameters as in Figure 2. Simulation was interrupted at an arbitrary time after the system had presumably settled to the attractor.

Hyperchaos was observed experimentally in the low-temperature avalanche break-down of p-Germanium [4]. The study suggested that the occurrence of hyperchaos in the experimental time series is closely connected to an increase in the available degrees of freedom via occurrence of mutually coupled subsystems. The results of the semiconductor experiment were modeled with systems similar to (3) (see e.g. [5]) but the transition from chaos to hyperchaos could not be explained in terms of this model. In a chemical context, hyperchaos was found during catalytic CO oxidation on a Pt(110) single crystal surface [6]. As in the case of semiconductor instabilities, the transitions from periodic to chaotic to hyperchaotic dynamics was found to be linked to spatio-temporal pattern formation. Interestingly, in both experiments spatio-temporal turbulent states have been observed at different sets of parameters. It is tempting to investigate whether the present qualitative model of chaotic hierarchy in reaction-diffusion systems is applicable to these results.

[1] O. E. Rössler, Z. Naturforsch. **31a,** 1168 (1976).
[2] O. E. Rössler, Phys. Lett. A **71,** 155 (1979), O. E. Rössler, Z. Naturforsch. **38a,** 788 (1983).
[3] G. Baier, J. S. Thomsen, and E. Mosekilde, J. Theor. Biol. **165,** 593 (1993).
[4] R. Stoop, J. Peinke, J. Parisi, B. Röhricht, and R. P. Huebener, Physica D **35,** 425 (1989).
[5] B. Röhricht, J. Parisi, J. Peinke, and O. E. Rössler, Z. Phys. B: Condensed Matter **65,** 259 (1986).
[6] M. Eiswirth, Th.-M. Kruel, G. Ertl, and F. W. Schneider, Chem. Phys. Lett. **193,** 305 (1992).